IEICE Communications Express, Vol.13, No.9, 379–383

ComEX

LETTER

Evaluation of shadowing effect on channel observation for spectrum sharing access

Hideya So [1, a)] **and Hayato Soya** [2]

Abstract Spectrum sharing, in which multiple wireless systems share the same radio resources, has been considered to improve frequency utilization efficiency. As a spectrum sharing without control signals, a technique that observes the usage of radio resources, called channel occupation ratio, used by other systems and selects a vacant channel has been considered. However, previous studies have simplified the model of the interfering system, which is different from the real environment. In wireless communications, fluctuations in received power occur due to shadowing caused by the location and the surrounding environment. Previous studies have not clarified the effect of received power fluctuation due to shadowing on observing the occupancy rate. This letter formulates the effects on the observation results of received power fluctuations due to the location of interfering stations and shadowing. Computer simulations with randomly placed interfering stations and shadowing environments show that the proposed formulation almost matches the observed results.

Keywords: spectrum sharing, interfering system, shadowing, channel observation, channel occupation ratio

Classification: Wireless communication technologies

1. Introduction

The traffic demand for mobile communications has been increasing yearly due to the spread of smartphones [1]. In mobile communications, the fifth-generation mobile communications system (5G) service will start around 2020, and the next-generation mobile communications system (6G) has also begun to be considered [2]. In addition to the high-speed and large-capacity communications studied, 5G has established new axes, such as multi-terminal connectivity and highly reliable, low-latency communications, and is being considered for various use cases [3]. 6G aims to extend 5G further and requires advanced wireless control to expand coverage, including the airspace, and to realize cyber-physical convergence. Cyber-physical fusion requires much information to be exchanged between wearable devices and sensors. Therefore, the number of devices is expected to increase, and the communications requirements are expected to expand accordingly.

Although the use of millimeter-wave bands has been considered to achieve high-speed and large-capacity communications, regarding the degradation caused by human shielding, the use of microwave bands is preferable for the use of a huge number of devices. On the other hand, the microwave band is used by a variety of wireless systems, and only a few available frequencies can be newly allocated. It is essential to develop technologies to improve spectrum utilization efficiency to utilize the microwave band in the future.

Spectrum sharing, in which multiple wireless systems share the same frequency band, is expected to be a technology that improves spectrum utilization efficiency [4]. If the terminals in a wireless system always have a full buffer, they can use 100% of the radio resources. However, since the communications demands of the terminals vary depending on the application and usage, there may be free radio resources depending on how they are used. Spectrum sharing reduces free radio resources and improves spectrum utilization efficiency by sharing radio resources such as time/frequency/space among multiple wireless systems. To achieve spectrum sharing, the management system must manage/allocate the radio resources used by all the shared systems [5]. However, as the number of shared systems increases, the number of control signals increases, resulting in lower spectrum utilization efficiency. Therefore, this research aims to establish an autonomous spectrum-sharing technology that does not require a management system.

When multiple systems share radio resources through autonomous control, radio interference between the systems becomes a problem. To avoid radio interference, real-time observation of radio resource usage and determination of low-usage radio resources based on the observation results are being considered [6]. Here, a frequency among the radio resources is defined as a channel, and the channel occupancy ratio (COR) is defined as the percentage of time that other radio systems use the channel. By observing the COR of all available channels and selecting the channel with the lowest COR, mutual interference can be reduced, and communications can be performed.

Due to the limitation of the number of RFs in the observer, the COR is observed by switching the channels sequentially [7]. If the time to observe the COR for each channel is made longer, the observation accuracy of the COR improves, but the time available for communications relatively decreases [8]. On the other hand, a short observation time decreases the observation accuracy, which increases the probability of selecting a channel with a high COR, increasing interference. Therefore, we have revealed that the observation accuracy and system throughput can be improved by dividing the observation interval into two parts

[1] Department of Electrical and Electronic Engineering, Shonan Institute of Technology, Fujisawa, Kanagawa 251–8511, Japan
[2] Department of Applied Information Engineering, Suwa University of Science, Chino, Nagano 391–0292, Japan
[a)] so.hideya@m.ieice.org

DOI: 10.23919/comex.2024XBL0106
Received May 28, 2024
Accepted June 14, 2024
Publicized July 9, 2024
Copyedited September 1, 2024

and excluding the channel with high COR from the second observation based on the first observation result [9].

The observed COR's standard deviation has been considered a reliability indicator of COR observation accuracy [10]. The longer the observation time becomes, the smaller the standard deviation, so the error between the observed and the true COR is small. In [10], the standard deviation of the observed COR using the observed interference packet length is theoretically derived. However, the conditions for the interfering system were ideal. Since another study [9] does not consider the location of IUTs, there is an environment where signals from all IUTs can be observed. It also does not consider variations in received power due to shadowing. Shadowing causes the received power of the signal at the observer to vary depending not only on the location of the IUT but also on the surrounding environment. In other words, the effect of shadowing and IUTs' location on the observed COR's standard deviation has yet to be clarified in [10]. Therefore, this letter clarifies the observed COR's standard deviation, considering the location of interfering stations and variations in received power due to shadowing. This can guarantee the observed COR's accuracy and improve the throughput during channel selection control.

2. Observation of CORs considering shadowing

2.1 Observed COR

This letter assumes that Interfering User Terminals (IUTs) are within a distance $r_{\max}$ from an access point (AP). Although not shown in the figure, multiple User Terminals (UTs) connect to AP in the area. AP has an observer that measures the available channels' channel occupancy rate (COR). AP selects the channel with the lowest COR based on the observation results and communicates with UTs. The COR is calculated by the ratio of the sum of the signal times that exceed a certain threshold at the observer to the observation time. Let L be the number of IUTs, M_l be the number of observed signals from the l-th IUT, and $T_{\mathrm{P}}(l,m)$ be the time length of the m-th received signal from the l-th IUT. When the observer measures with an observation time of T_{OBS}, the observed COR, $\hat{\rho}$, is expressed as

$$\hat{\rho} = \frac{\sum_{l=1}^{L}\sum_{m=1}^{M_l} T_{\mathrm{P}}(l,m)}{T_{\mathrm{OBS}}}. \tag{1}$$

Assuming that T_{OBS} is sufficiently long and that all IUTs have similar characteristics, $\hat{\rho}$ can be approximated as follows:

$$\hat{\rho} \simeq \frac{L\lambda\overline{T_{\mathrm{P}}}}{T_{\mathrm{OBS}}}, \tag{2}$$

where $\overline{T_{\mathrm{P}}}$ is the average occupied time per transmission and λ is the average number of transmissions per IUTs. This means that the number of IUTs, the frequency of transmission of IUTs, and the time length per transmission determine the observed COR.

2.2 Observation with slots

In the case of a system using random access, such as Carrier Sense Multiple Access with Collision Avoidance (CSMA/CA), each IUT transmits its signal autonomously, so the transmission timing is different. When the number of IUTs is large or the transmission frequency is high, the timing at which DIFS starts counting is considered aligned because each IUT performs carrier sense. Therefore, to simplify this study, this letter assumes that each IUT synchronizes at the observation slots as shown in Fig. 1. In other words, there is no signal crossing the observation slots. If a signal of any IUTs can be observed in each observation slot, it is counted as being in the use of the channel. On the other hand, if no IUT is transmitting a signal, or if one of the IUTs sends a signal but cannot be observed by the IUT, it is counted as vacant. The observed COR is calculated by the ratio of the total number of slots in use to the total number of observed slots N.

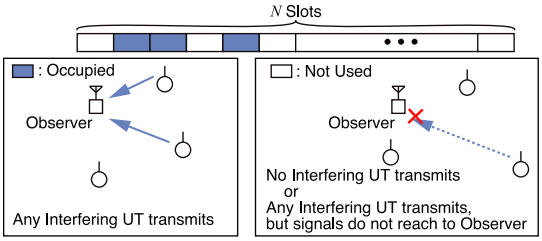

Fig. 1 Observation of COR using observation slots.

Each slot can be considered a binomial distribution since it is a transition model with two states: in and not in use. When the true value of COR is ρ, the probability of observed COR, $\hat{\rho}$, can be expressed as

$$p(\rho,\hat{\rho}) = \frac{1}{\sqrt{2\pi\sigma^2}}\exp\left(-\frac{(\hat{\rho}-\rho)^2}{2\sigma^2}\right) \tag{3}$$

[11]. σ is a standard deviation and can be expressed as

$$\sigma = \sqrt{\frac{\rho(1-\rho)}{N}}. \tag{4}$$

σ represents the observed COR spread, which is determined by the true COR ρ and the number of observed slots N.

2.3 Observation spread for shadowing

Equation (4) assumes that the observer can receive signals from all IUTs and does not consider the location of the IUTs. Therefore, the effect on the observed COR is considered when the received power fluctuates. The standard deviation σ_{prop} of the observed COR considering the received power fluctuation is extended from (4) as follows:

$$\sigma_{\mathrm{prop}} = \sqrt{\frac{\alpha\rho(1-\alpha\rho)}{\beta N}}, \tag{5}$$

where α is a coefficient that accounts for the increase in observation range due to shadowing, and β is a coefficient that accounts for the apparent decrease in observation time due to fluctuations in the number of IUTs. Since shadowing causes the received power to fluctuate, the observer can observe the signal from distant IUTs. In other words, the observation range increases with shadowing compared to the case without shadowing. Therefore, α is introduced as a coefficient to account for the increased observation range

due to shadowing. Since the locations of IUTs are randomly distributed, the number of IUTs observed changes depending on the location of each IUT. In addition, the number of IUTs that can be observed varies stochastically due to variations in received power caused by shadowing. The time it is required for the observed COR to converge increases due to the variation in the number of IUTs. Therefore, β is introduced as a coefficient that considers the change in observation time.

3. Computer simulation

3.1 Simulation conditions

Computer simulations that used MATLAB network simulation of the MAC layer were conducted to reveal the effect of shadowing on the observation results. The carrier frequency was set to 2.4 GHz, and 3D UMi Street Canyon NLOS [12] is used as the propagation model. The standard deviation of shadowing σ_{SF} was set to 7.82 dB. In the following simulations, σ_{SF} was set to 0 dB when shadowing was not considered. The antenna height of IUTs and observer are set to 1.5 m and 10 m, respectively. The transmit power and antenna gain of the IUTs were set to 23 dBm and 0 dBi, respectively, and were identical for all IUTs. Signal generation at the IUT was assumed to follow Poisson generation, and its parameter λ was assumed to be the same for all IUTs. The observer can observe the interfering signal when it is greater than −92 dBm. Note that the received power is averaged, and power variations within each signal are not considered in these simulations. IUTs' locations are assumed to be a uniform distribution of IUTs within a radius of r_{max} = 300 m centered at the observer, as shown in Fig. 2. The unit time length of the observation slot Δt was set to 0.1 ms. When multiple IUTs are transmitting in the same slot, the slot is observed as being in use.

3.2 Effect of shadowing on observation results

Figure 3 shows the standard deviation of the observed COR with the number of observed slots being a parameter. The true value of COR was set to $\rho = 0.31$, and no shadowing is assumed in this result. The spread of the observation results (standard deviation σ) can be reduced by increasing the number of observation slots N. Since the standard deviation variation slows down when the number of observation slots N exceeds 3000, the number of observation slots is set to $N = 3000$ in the following simulations.

The effect of shadowing, in which the received power fluctuates depending on the surrounding environment, such as obstacles, is evaluated. Figure 4 shows the average reception rate of signals as a function of the distance r between the observer and IUTs. Results with and without shadowing are shown for comparison. The average reception rate is the average of multiple IUTs at the same r with variations in received power due to different obstruction conditions. Without shadowing, the observer cannot receive signals from IUTs for $r > 240$ m. This is because the received signal power falls below the threshold value of −92 dBm due to distance attenuation. On the other hand, with shadowing, the reception rate gradually decreases for $r > 80$ m and can receive signals for $r > 240$ m. This is because the received power with shadowing takes different values for each IUT even if the distance between the observer and IUT is the same. The received power, P_{R}, can be expressed as

$$P_{\mathrm{R}} = P_{\mathrm{T}} + P_{\mathrm{PL}} + P_{\mathrm{S}}, \tag{6}$$

where P_{T} is the transmitted power, P_{PL} is the path loss determined by the distance between the observer and IUT, and P_{S} is the shadowing. Note that these simulations are not considered instantaneous variations due to multipath but assume that they are constant on average during the observation. This simulation assumes that P_{S} fluctuates according to lognormal Gaussian distribution with mean 0 dB and standard deviation $\sigma_{\mathrm{SF}} = 7.82$ dB. P_{S} can be negative values and takes different values for each IUT even if r is the same. The result in Fig. 4 is the average reception rate from multiple IUTs with the same r. So, the received power also fluctuates according to a lognormal Gaussian distribution. Therefore, for $r > 80$ m, the reception probability gradually decreases. It can be seen that shadowing can result in the reception of distant interfering signals in some cases and the inability to receive nearby interfering signals in other cases.

Figure 5 shows the standard deviation characteristics with λ of the IUTs being a parameter. Figure 5 (a) shows the

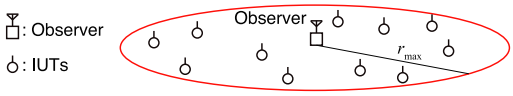

Fig. 2 Placement example of observer and IUTs.

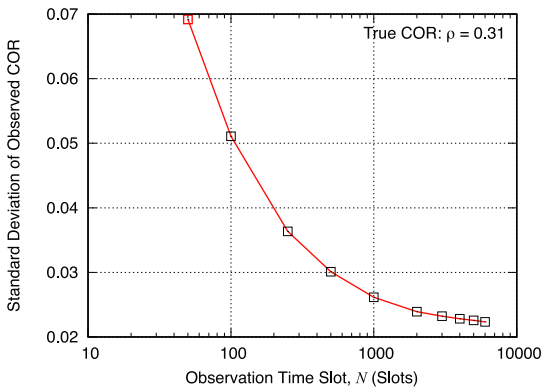

Fig. 3 Standard deviation of observed COR as a function of the number of observation slots, N.

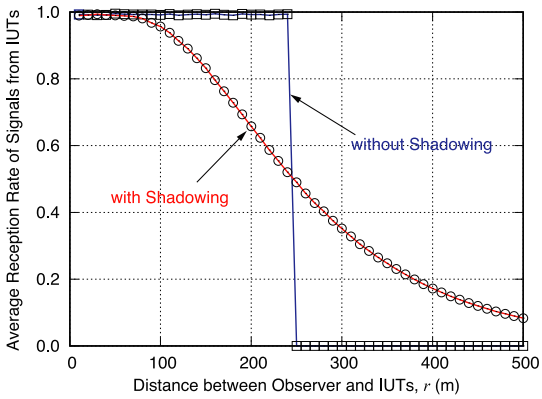

Fig. 4 The average reception rate relative to the distance between the observer and IUT.

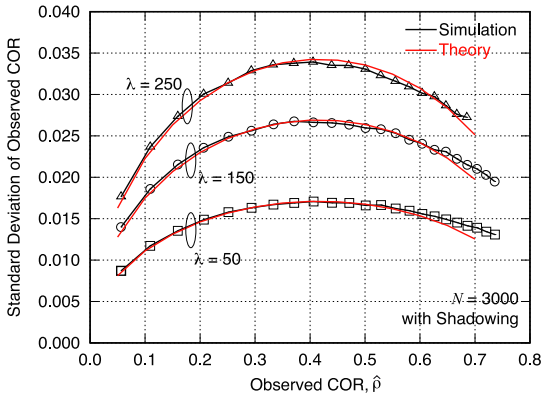

(a) With shadowing

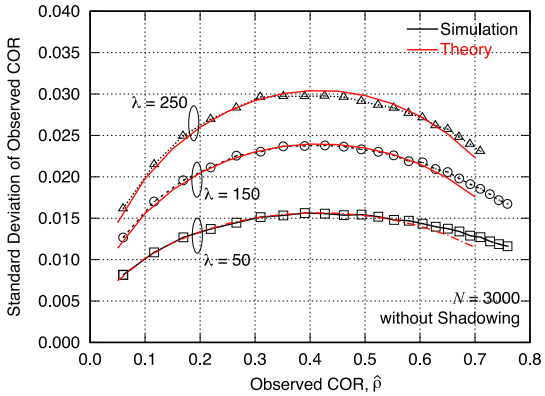

(b) Without shadowing

Fig. 5 Standard deviation characteristics of observed CORs.

Table I Values of β

λ	With shadowing	Without shadowing
50	0.28	0.34
150	0.12	0.15
250	0.07	0.09

characteristics with shadowing and Fig. 5 (b) shows the characteristics without shadowing. The standard deviation is about 1.1 times larger with shadowing than without shadowing. This is because the number of IUTs changes from observers due to shadowing, and the observed COR changes accordingly. In a dynamic environment where shadowing is expected, it is desirable to set the number of observation slots longer than usual because the variation of the observed COR is larger.

The respective theoretical values obtained by (5) are shown for comparison. The simulated values are almost the same as the theoretical values. All theoretical results were set to $\alpha = 1.2$. The observer can observe the signal without shadowing at distances greater than 240 m. With shadowing, however, the observer can observe. In this simulation, the area size was set to 300 m, meaning the observer can observe 1.25 (= 300/240) times larger areas with shadowing than without shadowing. On the other hand, because shadowing may prevent observation within 240 m, the coefficient of shadowing, α, is set to 1.2, which is smaller than 1.25. Note that α is considered dependent on the propagation model and area size.

β were set different for each results and summarized in Table I. β was obtained by fitting from simulation results. As λ increases, the observed COR and the standard deviation increase. It can be seen that β increases by a factor of 0.4 and 0.25 as λ is increased from 50 to 150 and 250, respectively. In an environment with shadowing, β is 0.8 times smaller than in the absence of shadowing. Therefore, with shadowing, the observer should increase the 1.25 times observation time to improve the observation accuracy.

4. Conclusions

For the reliability of the observation accuracy of Channel Occupation Ratio (COR) in spectrum sharing access, the effect of the location and shadowing of interfering stations (IUTs) on the observed COR is clarified. The location and shadowing of IUTs cause fluctuations in the received power of the interfering signal. This letter proposes an extension of the theoretical expression for the observation spread of the observed COR that takes these fluctuations into account. Computer simulations were evaluated to clarify the effects on the observed COR when the presence of shadowing and the amount of interference varied, and it was found that the proposed equation is in close agreement with the proposed equation.

Acknowledgments

This work was supported in part by JSPS KAKENHI Grant Number JP23K16874. The authors would like to thank S. Ohta for his technical assistance.

References

[1] Ericsson, "Ericsson mobility report," Nov. 2022.
[2] T. Nakamura, "5G Evolution and 6G," *VLSI-DAT 2020*, Sept. 2020. DOI: 10.1109/vlsi-dat49148.2020.9196309
[3] A. Osseiran, F. Boccardi, V. Braun, K. Kusume, P. Marsch, M. Maternia, O. Queseth, M. Schellmann, H. Schotten, H. Taoka, H. Tullberg, M. A. Uusitalo, B. Timus, and M. Fallgren, "Scenarios for the 5G mobile and wireless communications: the vision of the METIS project," *IEEE Commun. Mag.*, vol.52, no.5, pp. 26–35, May 2014. DOI: 10.1109/mcom.2014.6815890
[4] 3GPP TSG RAN Meeting #84 RP-191052, "Dynamic spectrum sharing in Rel-17," Newport Beach, CA, USA, June 3–17 2019.
[5] A. Ikami, T. Hayashi, and Y. Amano, "Interoperator channel management for dynamic spectrum allocation between different radio systems," *IEICE Commun. Express.*, vol. 9, no. 10, pp. 512–518, Oct. 2020. DOI: 10.1587/comex.2020xbl0106
[6] S. Takeuchi, M. Hasegawa, K. Kanno, A. Uchida, N. Chauvet, and M. Naruse, "Dynamic channel selection in wireless communications via a multi-armed bandit algorithm using laser chaos time series," *Sci. Rep.*, vol. 10, no. 1, Jan. 2020. DOI: 10.1038/s41598-020-58541-2
[7] T. Xiong, Y. Yao, Y. Ren, and Z. Li, "Multiband spectrum sensing in cognitive radio networks with secondary user hardware limitation: random and adaptive spectrum sensing strategies," *IEEE Trans. Wireless Commun.*, vol. 17, no. 5, pp. 3018–3029, May 2018. DOI: 10.1109/twc.2018.2805729
[8] G. Umashankar and A.P. Kannu, "Throughput optimal multi-slot sensing procedure for a cognitive radio," *IEEE Commun. Lett.*, vol. 17, no. 12, pp. 2292–2295, Dec. 2013. DOI: 10.1109/lcomm.2013.102613.131825
[9] H. So and H. Soya, "Two-step channel observation scheme considering spread of observation results in dynamic spectrum sharing," *IEEE Open J. Veh. Technol.*, vol. 3, pp. 367–374, July 2022. DOI: 10.1109/ojvt.2022.3192737
[10] H. So, H. Soya, and K. Fukawa, "Spectrum sensing scheme measuring packet lengths of interfering systems for dynamic spectrum

sharing," *IEEE Access*, vol. 9, pp. 135160–135166, Oct. 2021. DOI: 10.1109/access.2021.3116951

[11] H. Soya, O. Takyu, K. Shirai, M. Ohta, T. Fujii, F. Sasamori, and S. Handa, "Fast rendezvous scheme with a few control signals for multi-channel cognitive radio," *IEICE Trans. Commun.*, vol. E101-B, no. 7, pp. 1589–1601, Jan. 2018. DOI: 10.1587/transcom.2017cqp0022

[12] 3GPP TR 38.901 V14.3.0, "Study on channel model for frequencies from 0.5 to 100 GHz," Jan. 2018.